Lab on a Chip

Dynamic Article Links ▶

FOCUS

Acoustofluidics 12: Biocompatibility and cell viability in microfluidic acoustic resonators

Martin Wiklund*

Manipulation of biological cells by acoustic radiation forces is often motivated by its improved biocompatibility relative to alternative available methods. On the other hand, it is well known that acoustic exposure is capable of causing damage to tissue or cells, primarily due to heating or cavitation effects. Therefore, it is important to define safety guidelines for the design and operation of the utilized devices. This tutorial discusses the biocompatibility of devices designed for acoustic manipulation of mammalian cells, and different methods for quantifying the cell viability in such devices.

Department of Applied Physics, Royal Institute of Technology, SE-10691, Stockholm, Sweden. E-mail: martin@biox.kth.se; Tel: +46 8 5537 8134

I Introduction

Devices for acoustic manipulation of particles and cells typically utilize the acoustic radiation force[1] acting on suspended objects. This force is stronger if the acoustic field is of standing-wave type and of high frequency (>MHz), and is thus in the ultrasound regime. When handling biological cells it is important to know if the acoustic field is capable of causing any stress or damage to them. Generally, acoustic energy is of mechanical nature in the form of vibrations and pressure fluctuations, *i.e.* it consists of kinetic and potential energy. Therefore the acoustic field may cause "shaking" and "squeezing" effects on the cells. In a plane-propagating wave, the shaking and squeezing effects are equally large anywhere in the wave. In a standing wave, however, there is a phase difference between the maximum vibration and maximum pressure leading to a spatial separation between the velocity antinodes and the pressure antinodes, respectively. For that reason, it is important to consider not only the energies or pressure/velocity amplitudes, but also the types of acoustic fields (*e.g.* standing or propagating waves) and the position of cells in that field, when investigating the

Martin Wiklund is an Associate Professor in applied physics at the Dept. of Applied Physics, Royal Institute of Technology (KTH), Stockholm, Sweden. He received his M.Sc. in engineering physics from Lund University in 1999 and his Ph.D. in physics from the Dept. of Physics, KTH, Stockholm, in 2004. In 2004–2005, he was a postdoctoral fellow at the Fraunhofer Institute for Biomedical Engineering (IBMT), Berlin, Germany. He returned to KTH in 2005, becoming an Assistant Professor in 2006, and Associate Professor in 2009. Currently, Wiklund's research is focused on acoustic and optical methods for micro-scaled handling and characterization of cells, and applications of the methods to biomedical research. He is also a lecturer in various courses in basic physics, optics, ultrasound physics and diagnostic ultrasound. He is author to >20

Martin Wiklund

peer-reviewed journal papers, >50 conference contributions including >20 invited talks, two patents and a recent book chapter ("Ultrasonic Manipulation of Single Cells", in Single-Cell Analysis: Methods and Protocols, Methods in Molecular Biology, vol. 853, Springer, 2012).

Foreword

In the twelfth paper of 23 in the *Lab on a Chip* Acoustofluidics tutorial series, Martin Wiklund discusses the bioeffects on cells in microfluidic acoustic resonators. It is widely known that ultrasound can be used to damage cells, such as in cell disruptors, which raises the question of whether ultrasound affects cells in acoustofluidic systems as well. Acoustic effects, such as thermal and streaming effects, cavitation, and effects from the acoustic radiation forces are discussed, and additionally, conditions under which these can be harmful to cells are identified. Methods for measuring the ultrasonic impact on cells in terms of viability are also covered.

Andreas Lenshof – coordinator of the Acoustofluidics series

impact on cell viability. Furthermore, the time constant of the fluctuations, *i.e.* the frequency, is important; typically cavitation is more likely to occur in the low ultrasound frequency regime (<1 MHz), while absorption leading to heating increases with frequency.

Many past studies of the bioeffects of ultrasound (*i.e.* any observable biological effect that is likely caused by ultrasound) are related to ultrasonography, or ultrasonic (medical) imaging. This is of interest since the acoustic energies and frequencies employed in ultrasonic imaging are comparable in magnitude to the ones used in acoustic manipulation of cells in micro-devices. Ultrasonic imaging has been used for about half century[2] and is the most widely used diagnostic imaging tool in clinics around the world. The general conclusion is that no epidemiological evidence exists of any adverse effects in humans caused by routine use of diagnostic ultrasound.[3,4,5] However, as pointed out by Barnett *et al.*,[5] any past safety record should not be mistaken for a guarantee that harm can never occur. This general advice is also applicable when using micro-devices for the ultrasonic manipulation of cells. It is important, however, to note that there might be different bioeffects in the human body compared to an *in vitro* cell culture in a micro-device when using similar acoustic field parameters, and these effects might vary between different cell types. Therefore, a general guideline is that the cell viability is difficult to model and predict; it needs to be experimentally investigated for each device and for each cell type used.

Several ultrasound applications exist where an adverse effect on cells or tissue is intended. For example, shock-wave lithotripsy and high-intensity focused ultrasound (HIFU) are ultrasonic methods used for, *e.g.*, destroying kidney stones, gall stones and similar. This therapeutic ultrasound technology, sometimes called ultrasound surgery, has also been used for creating localized haemostasis to prevent internal bleeding as well as tissue necrosis for cancer therapy without damaging nearby tissue.[6] The mechanisms involved are complicated but typically involve heating combined with bubble activity (cavitation) at acoustic intensities in the range 10^3–10^4 W cm^{-2}.

Furthermore, a common laboratory method is to lyse cells in suspension by "sonication" in an acoustic field in the low-frequency ultrasound regime, typically at 30–50 kHz. This method is well known among cell biologists, but should not be mistaken for ultrasound activity in general since the lysing effect is based on cavitation, which is more likely to occur at lower ultrasound frequencies.

In this focus, the physical mechanisms of ultrasound capable of causing various bioeffects on cells are discussed. The scope of the paper is primarily limited to devices for ultrasonic standing wave manipulation of mammalian cells. Micro-scaled devices are highlighted, but the paper also discusses macro-scaled devices since many important and relevant studies were performed in larger systems. The physical mechanisms of interest can be divided into thermal and non-thermal effects. Here, cavitation is the most important non-thermal effect, but other non-thermal effects, such as acoustic radiation forces and acoustic streaming, are also discussed. Furthermore, different observed bioeffects on cells are discussed as well as different available methods to quantify the impact of ultrasound on cell viability.

II Physical mechanisms of ultrasound causing a bioeffect

This section discusses the origin of different physical mechanisms of ultrasound affecting cells and tissue, and provides a few design criteria important for controlling or improving the biocompatibility of an ultrasonic manipulation device.

A Thermal effects

When ultrasound is absorbed by a material the mechanical energy is primarily converted into heat. However, the high-Q resonators used for ultrasonic manipulation of particles and cells are typically made of low-loss materials such as silicon, glass, steel and a water-based suspension. Therefore the absorption of ultrasound is very small, in particular for frequencies in the range ∼1–10 MHz. On the other hand, temperature elevation remains a problem in ultrasonic manipulation devices. There are two reasons for this: (1) Heat is generated from electromechanical losses in the piezoelectric layer in the

transducer and (2) heat losses in the thin glue layers in between the different supporting solid layers in the resonator. The localized heat generated primarily in the transducer and glue layers may then be conducted to the fluid and cells in the channel/chamber of the resonator causing a thermal bioeffect. Care should also be taken if polymers are used as supporting layers. However, it is not commonly used in ultrasonic particle manipulation devices due to its high heat losses.

When discussing the bioeffects of ultrasound, it is important to distinguish between local and global effects, as well as between short and long-term effects. Let us first briefly consider what happens when the temperature is elevated in the human body (*i.e.* globally). Regardless of what caused the heating (whether it is fever or hyperthermia), a temperature increase of only a few degrees activates a signaling pathway, eventually resulting in a transient expression of heat shock proteins (HSPs). HSPs are important for retaining the functions of other proteins in the cell, *e.g.* by assisting temperature-sensitive processes such as transport and folding of proteins.[7] Here, the time scale is important; mechanisms involving HSPs have a time constant of several minutes,[8] while ultrasound-induced heating often has a time constant of seconds. This means that the body cannot defend itself against such rapid temperature increase. As a guideline for humans, an elevated and retained full-body temperature in the range 40.5–41.5 °C is dangerous, and above 41.5 °C potentially fatal. For local hyperthermia, the threshold temperature for irreversible damage in several tissue types was found to be about 43 °C, for skin 47 °C with erythema and pain, 55 °C during 40 s caused blistering and 60 °C during 60 s caused necrosis.[5] A general model predicting the bioeffect of ultrasound at different temperatures was developed by Sapareto and Dewey.[9]

In vitro cell lines generally have a wider range of tolerable temperatures compared to whole organisms. For example, cryopreservation is a widely used technique for cell storage at very low temperatures. Furthermore, a lethal temperature for a whole organism may be tolerable for an individual cell.[5] However, the heat shock response takes place on the molecular level and is therefore also

applicable to individual cells. The reason for the relatively moderate temperature increase needed to trigger a heat shock response (a few degrees) is the high dependence of protein stability on the temperature. Protein conformation – critical for the function of the protein – is optimized within a very limited temperature interval. Therefore, a small change in temperature may lead to conformational changes, protein misfolding, entanglement and/or unspecific aggregation of proteins. These effects may cause a variety of different cellular responses, of which the most apparent is cell cycle arrest and a stagnation of the growth rate.[7] Other reported effects are cytoskeletal defects due to actin filament reorganization and misplacement or fragmentation of organelles.[10] Thus, although the cell may be technically viable (*e.g.* having an intact cell membrane) its functions and internal structure may be severely affected by a moderate increased temperature.

Temperature effects and recommendations for human cells are summarized schematically in Fig. 1. A rough guideline for most mammalian cells is that cell growth is optimal at 37 °C but often

tolerable between 33–39 °C. If the temperature exceeds ∼43 °C cell death is most likely, and above 45 °C proteins become denatured. Between ∼39–43 °C, the bioeffect is highly diverse and dependant on a variety of factors, including cell type, heating rate, and time of retained and elevated temperature. In addition to the production of heat shock proteins, typical effects in this temperature interval include increased metabolic activity and cell cycling rates. On the other hand, at sub-physiological temperatures (∼33–37 °C), the cellular response is also diverse depending on cell type and system. Al-Fageeh *et al.*[11] reviewed the "cold shock" response in cultured mammalian cells, which typically leads to a modulation of the cell cycle, metabolism, transcription translation and the cell cytoskeleton. He pointed out that the bioeffects at subphysiological temperatures does not necessarily have to be inhibitive or detrimental. For example, reports exist where the production of recombinant proteins is increased at lower temperatures.[11] However, for most mammalian cell lines the proliferation ceases

although the viability is prolonged at lower temperatures.[11,12] This eventually results in slow cell death if the temperature is kept below approx. 33 °C for prolonged times. On the other hand, since the metabolic rate typically decreases with decreasing temperature, cells are more sensitive to changes in nutrient and oxygen supply at 37 °C than at lower temperatures.

In summary, what is the recommended temperature when using ultrasound as a manipulation tool for mammalian cells? Naturally, it is to keep the system at the physiological temperature 37 °C with a tolerance of about ±1 °C. This will reduce the risk of ultrasound-generated heat variations interfering with any measured cellular process of interest. The recommended tolerance of ±1 °C is also in line with the safety definition used for ultrasonic medical imaging. In medical imaging, the thermal index (TI) is used as an international standard, and is defined as the power produced by the transducer divided by the power needed to raise the temperature 1 °C. Thus, TI = 1 means that there is a risk of heating the examined tissue by approximately 1 °C.
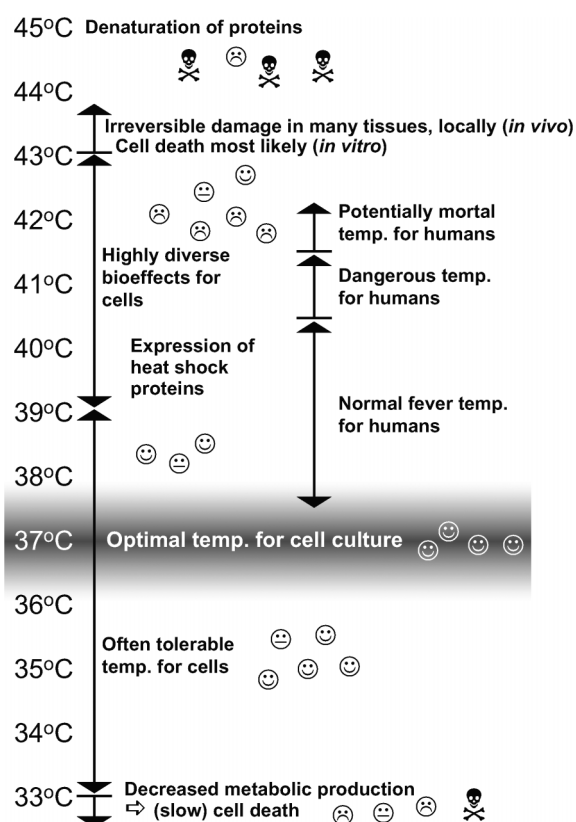

Fig. 1 Overview of the temperature dependence of different observed bioeffects in humans and for mammalian cells.

If TI > 1, the operator should carefully consider the benefits of the examination relative to the risks. Concerning resonators for ultrasonic particle manipulation, there is an additional advantage of controlling the temperature. A stable temperature will also improve the resonance stability by keeping the temperature-dependent acoustic wavelength constant. Thus, both the ultrasonic manipulation performance as well as the cellular environment benefit from a controlled and constant temperature.

A few different strategies have been reported for temperature regulation in ultrasonic standing-wave manipulation devices. One method is to cool the system by a water loop,[13] a fan[14] or a Peltier element[15] close to the piezoelectric layer, see Fig. 2. A water loop is suitable as a heat sink for large-scale devices, while a Peltier element is better for miniaturized devices. Furthermore, a Peltier element is the most sophisticated method since it can be used for either cooling or heating depending on the ultrasonic power needed. Another method is based on utilizing the heat generated by the ultrasonic device, typically in the transducer, in an active temperature-regulation scheme.[16,17] For example, provided that the ultrasound-generated heat does not lead to an increase of more than 10–15 °C, the temperature will not exceed 37 °C if the device is operated at room temperature. For smaller temperature increases, the ultrasound-generated heat can be combined with an external heating system such as a heatable chip holder or a hood with controlled air environment.

In this way the total temperature increase can be tuned so that the final temperature is kept at 37 °C. The latter method can, of course, only be used if the temperature increase due to ultrasound is moderate and will not lead to a total temperature exceeding 37 °C, otherwise a Peltier element should be used. The monitoring of the temperature can be performed using a thermocouple probe attached to a suitable location on the chip, for example (see Fig. 2), or by measuring the temperature-dependent fluorescence intensity from Rhodamine B.[18] The latter method has the advantage of monitoring the temperature directly at the location of cells, but the method is not as accurate as a thermocouple probe. In a fully temperature-controlled and CO$_2$-controlled micro-device, Vanherberghen et al. showed that human immune cells (B cells) were kept viable for up to 3 days of continuous ultrasonic exposure at relevant pressure amplitudes needed for trapping and retaining cells in well-defined clusters in a multi-well microplate.[17] This study is of interest since it confirms the high biocompatibility reported in commercially available macro-scaled ultrasonic manipulation devices, e.g. the SonoSep^{TM} and BioSep^{TM} systems by Applikon Biotechnology (Schiedam, The Netherlands).[19]

B Cavitation-based effects

Apart from thermally induced bioeffects, the other important effect to consider is cavitation-based effects. Cavitation is a physical phenomenon that can be induced by different means, of which ultrasound is one.[20] It can be defined as the formation and/or activity of gas/vapour filled cavities, i.e. bubbles, in a fluid medium. Such bubbles are efficiently formed and driven by low-frequency ultrasound, typically in the 20–200 kHz range. For example, a commercial ultrasonic cleaner used for cleaning, degassing, cell lysis etc. operates at around 30–40 kHz. However, many reports show clear cavitation effects for frequencies as little as approximately one or a few MHz.[5] Thus, there is no guarantee that cavitation will not occur even in the standard frequency range used for ultrasonic manipulation devices, i.e. 1–10 MHz. The stimulated bubble activity is classified as (1) stable cavitation and (2) inertial or transient cavitation. The first class, stable cavitation, is defined as the continuous oscillation of bubbles over a large number of cycles driven by the pressure fluctuations of the applied acoustic field. This type of cavitation typically produces highly localized acoustic streaming which may cause shear stresses on a nearby cell. The bioeffects are usually minimal but the presence of vibrating bubbles often completely destroys attempt to aggregate cells in a standing wave. The other class, inertial cavitation, is defined as a transient type of cavitation where the bubble oscillates heavily over a single or a few cycles, eventually leading to a violent collapse/implosion. The collapse is associated with localized high pressures and temperatures and high-velocity liquid jets. Typical scales of the parameters involved are >1000 °C temperature formed during 1 µs in a region of size
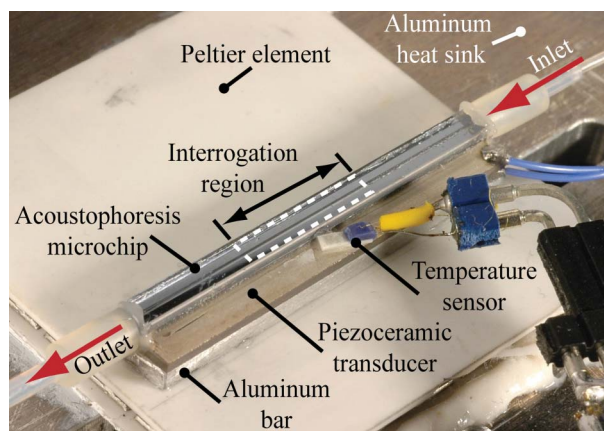

Fig. 2 The temperature-controlled acoustophoretic chip by Augustsson et al.[15] based on a Peltier element. The chip, piezo transducer (PZT), aluminum bar and Peltier element were sandwiched and glued together on a microscope stage. A Pt100 thermoresistive element was glued onto the PZT for feedback to the temperature control loop. The figure is reproduced from Ref. 15 with permission from The Royal Society of Chemistry.

~10 μm leading to internal pressures of 10–100 MPa (100–1000 atmospheres). Naturally, this is not a good environment for cells. The motion of the bubble surface is most often asymmetric, in particular for bubbles close to a rigid boundary, which may lead to directed liquid jets towards the surface. As a rough measure, bubbles that grow to more than twice their initial size within one or two cycles undergo inertial cavitation; otherwise stable cavitation is more likely.

The threshold for obtaining cavitation is very important for cell viability considerations. This threshold is dependent on both frequency and amplitude of the acoustic wave. However, even more important for the threshold is the presence of potential cavitation nuclei in the fluid in the form of dissolved or undissolved gasses and helping solid surfaces. This is similar to the process of heating water to the boiling point in a pan or pouring beer into a glass; bubbles are typically formed in the irregularities/crevices on the inside surface of the pan or glass. Thus, a general guideline to reduce the risk of bubbles in microfluidics is to use smooth, clean surfaces and degassed fluids (and non-permeable chip and tubing materials). If no helping surface or dissolved gasses are present, bubble creation and growth starting in the sub-micrometer domain is difficult. The reason for this is the high tension associated with the curved surface of a very small bubble; a tension of 100 MPa (1000 atmospheres) corresponds to the spontaneous creation of a bubble of radius 1.4 nm at room temperature in water.[21]

On the other hand, this theoretical calculation does not reflect reality since such pure fluids are difficult to produce. Still, it is important to reduce the amount of potential cavitation nuclei in the sample, e.g. by degassing the medium buffer with an ultrasonic cleaner before adding the cells. Apfel and Holland theoretically investigated the threshold acoustic pressure amplitude for obtaining inertial cavitation as a function of the size of pre-existing gaseous nuclei in water and other fluids for different ultrasonic frequencies.[22] Such pre-existing nuclei are typically microscopic pockets of undissolved gasses and/or vapour, which can easily be stabilized in the fluid on solid helping surfaces. Their results are shown in Fig. 3. As predicted by theory, the threshold pressure is high for nuclei-free or nm-sized nuclei fluid media. In such media, cavitation would practically never occur. On the other hand, if gaseous nuclei with sizes in the 100 nm–1 μm range are present in the fluid, the threshold pressure is within realistic levels often employed in acousto-fluidic applications. This pressure level is typically 0.1–1 MPa (corresponding to 1–10 atmospheres). We also note that for these pressures it makes a significant difference if the device is operated close to 1 or 10 MHz. From a cavitation perspective, 10 MHz is safer as near this frequency there is both a higher level of minimum threshold pressure as well as a steeper curve for larger nuclei sizes, compared to at ~1 MHz. The latter means that for a pressure exceeding the minimum threshold, a wider range of nuclei sizes will cavitate at 1 MHz than at 10 MHz.

In analogy to the thermal index (TI) used to estimate the risk of sample heating in ultrasound imaging, an international standard exists for estimating the risk of sample cavitation. This index is called mechanical index (MI) and is defined as the ratio of the (negative) peak pressure of the acoustic wave (in MPa) and the square root of the acoustic frequency (f, in MHz), i.e., $MI = P_{neg.peak}/\sqrt{f}$. A general guideline is to avoid $MI > 1$, which, if we compare with the predicted threshold pressure in Fig. 3, assumes a relatively nuclei-free sample (no bubbles larger than 100 nm present). Furthermore, from the MI definition, we expect the risk of cavitation as $\propto f^{-0.5}$. This is a good approximation for most relevant biological fluids and soft tissue. A more detailed theoretical study was performed by Apfel and Holland[22] who predicted the cavitation risk as $\propto f^{-0.60}$ for blood and $\propto f^{-0.48}$ for water, see the lower panel in Fig. 3.

If cavitation occurs in a cell suspension, severe physical and biological damage may occur. For stable cavitation, the most likely effect is cell membrane rupture, caused by shear stresses from microstreaming.[23,24] The effects of inertial cavitation can be more violent, including extreme temperatures, stresses and liquid jets, leading to direct cell destruction and death. Because of the high temperatures associated with inertial cavitation it is often difficult to distinguish pure cavitation effects from thermal effects. Despite this, a number of biological consequences of cavitation have been reported, e.g. necrosis[25] and strand breaks in DNA.[26] The reason for the latter is the high local energies associated with inertial cavitation, comparable in magnitude with ionizing radiation. A related field is called sonochemistry, where inertial cavitation is used for enhancing chemical reactions, e.g. by the production of free radicals which may catalyze reactions.[27] On the other hand, there also exist reports on beneficial bioeffects of cavitation. From stable cavitation, controlled microstreaming can lead to enhanced fluid stirring possibly beneficial for the transport of nutrients or enhanced blood perfusion.[23] Another field is the use of drug-loaded microbubbles for targeted imaging and therapeutics.[28] Furthermore, a cavitation-based technique for controlled and reversible membrane rupture is called sonoporation.[29] This is a technique where pulsed-mode cavitating microbubbles added to a cell sample temporarily create cell membrane pores, which increases the transmembrane permeability, followed by membrane recovery/repair.[30] Sonoporation has been suggested as an attractive method for drug delivery and cellular uptake of, for example, large molecules that otherwise cannot penetrate the cell membrane.[31] However, the method should be used with caution; although sonoporated cells normally recover and remain viable,[32] a recent study shows that sonoporation can lead to an arrest in the cell cycle and/or apoptosis, possibly due to a disturbance of the intracellular calcium ion concentration.[33] In another study, Carugo et al. demonstrated a microfluidic device for micro-bubble-free sonoporation.[34] The device was operated at resonance ~2 MHz and voltages between 0 and 40 V_{pp}, and was suggested to provide a simpler and more gentle methodology for drug delivery and uptake.

C Effects of acoustic radiation forces

Steady-state radiation forces are central for this tutorial topic since they are the basis for any acoustophoretic action on particles and cells. In standing-wave fields where the size of the cell is much smaller than the acoustic wavelength, the direct effect is clumping/aggregation of cells in bands at half wavelength intervals. This phenomenon is covered in more detail in other parts of this tutorial series.
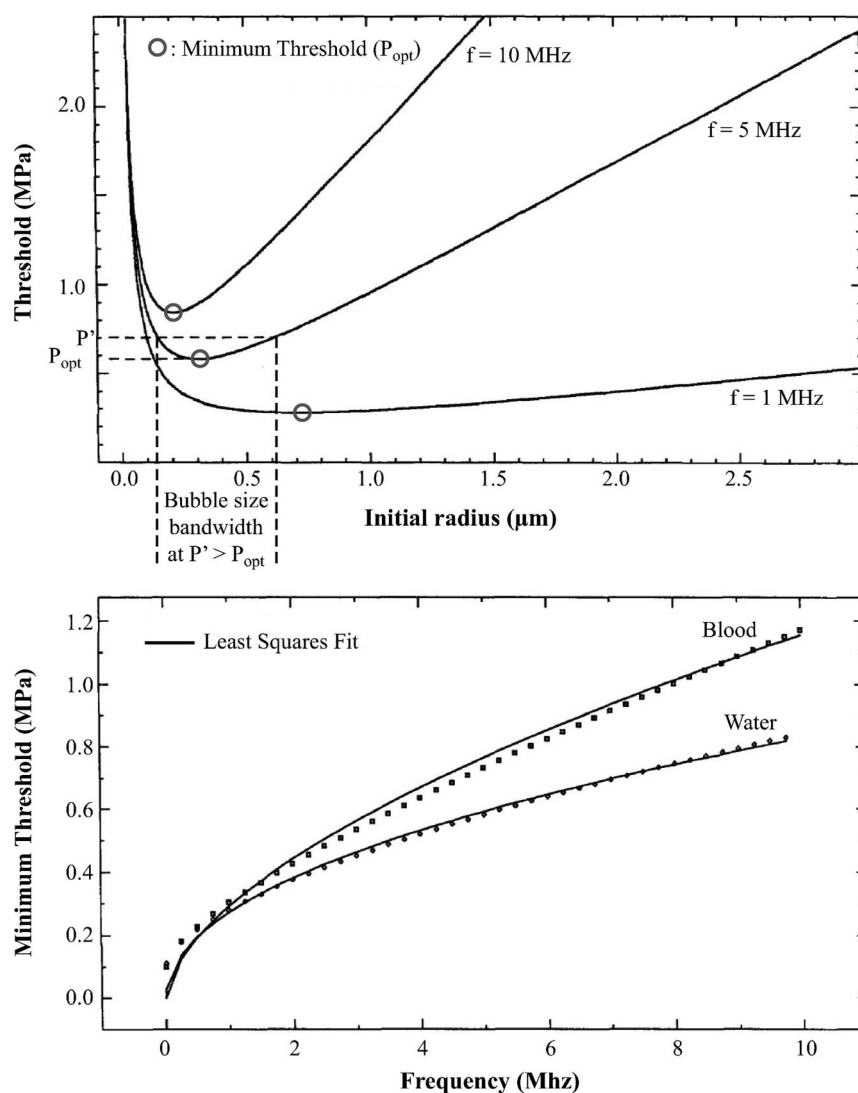
Fig. 3 Prediction of cavitation threshold levels. Upper panel: calculation of the cavitation threshold in water as a function of the size of pre-existing inertial cavitation nuclei (modeled as air bubbles in room temperature) for three different driving frequencies. P_{opt} is the lowest threshold for the optimal bubble size, and P' marks the bubble size bandwidth for a given pressure $> P_{opt}$. Lower panel: The calculated minimum threshold pressure, P_{opt}, for the optimal bubble size in the upper panel is plotted as a function of frequency (f) for two different fluids: blood and water. Least squares fits are made to the theoretical data, indicating that the threshold pressure is $\propto f^{-0.60}$ for blood and $\propto f^{-0.48}$ for water. The figure is reconstructed from Apfel and Holland[22] with permission from Elsevier.

In the early 1970s, Dyson et al. observed the reversible arrest of red blood cells in vivo in blood vessels of a living chick embryonic tissue due to ultrasonic standing wave exposure.[35] Actually, this work can be considered to be the first demonstration of acoustic trapping in a microfluidic system, approximately three decades before the technology was implemented in lab-on-a-chip devices. Bioeffects of in vivo red cell arrest is blood stasis, which may cause similar effects as for thrombosis.[36] The authors noticed a strong dependence of the blood cell arrest on the blood vessel orientation relative the orientation of the

utilized ultrasonic resonator, and suggested that for imaging applications, potential stasis could be minimized by continuously moving the ultrasonic probe during an examination. They also observed occasionally that some blood vessel endothelial cells were damaged in the plasma membranes on the luminal surface, resulting in cell debris and membrane fragments leaking out into the vessel cavity. Red cells were observed to sometimes adhere to these damaged spots in the endothelial membrane and could lead to sites of irreversible stasis and thrombus formation. However, it should be noted that the latter finding

was rare and had unknown causes, most probably not a direct effect of the radiation force but rather due to cavitation. Another study that has received some attention shows a correlation between ultrasonic exposure and the dislocation of neurons in the developing brain of fetal mice.[37] These authors showed that upon >30 min of ultrasound exposure at clinically relevant levels, some cortical neurons failed to reach their correct final position in the superficial gray matter of the brain when migrating from their site of development deeper inside the brain. The authors argued that it was unlikely that heating

or cavitation was involved; instead they suggested that acoustic radiation forces or microstreaming could be the reason for the disturbed neuron migration. However, it should be mentioned that the conclusions from this study are not applicable to humans due to their larger brain mass and brain developing times compared to mice.

D Effects of acoustic streaming

Since it is well-known that shear stresses from a fluid flow can cause membrane rupture and cell lysis,[38] it is not surprising that acoustic streaming could be a potential source of cell damage. Hughes and Nyborg verified this already in the 1960s in a work where bacteria, protozoa and erythrocytes were damaged by acoustic microstreaming from an 85 kHz vibrating tip.[39] However, the bioeffect of streaming depends largely on the magnitude of flow velocity; moderate steaming may cause beneficial stirring and fluid exchange effects[23] or lead to mechanically activated cell signal pathways.[40] Good examples of the benefits of fluid exchange are microfluidic perfusion cultures, where controlled delivery and removal of soluble factors are used for defining microenvironments at the level of single cells.[41] Generally, streaming-based effects have a much lower pressure threshold than the other effects discussed in this section; typical shear stresses causing a bioeffect are in the low kPa range or even lower.[5,38]

E Effects not caused by ultrasound

When handling cells in a micro-scaled device, other effects than ultrasound may be of interest for the biocompatibility. Most important is the choice of material facing the microchannel/microchamber, particularly if cells are in contact with this material. Many of the standard materials used in microfabrication technology have been successfully implemented in micro-scaled cell culture systems. Examples include polydimethylsiloxane (PDMS), silicon, glass and polymethylmethacrylate (PMMA), or combinations of such materials.[41] Since glass is a reliable material in standard bulk cell cultures it is straightforward to use for microscaled devices. However, in microfluidic perfusion cultures PDMS is the most popular material. One reason for this is its gas permeability, a property not

valid for silicon or glass. On the other hand, PDMS is a lossy and weakly reflecting material and is therefore not suitable in an acoustic resonator unless used only as a passive spacer.[17,42] Additional challenges with PDMS are its high hydrophobicity and permeability for organic solvents. Thus, glass and silicon are recommended as the first choice for biocompatible ultrasonic cell handling in chips.[17] Other material aspects to consider when handling cells for extended periods of time include the use of bio-coated materials for facilitating cell adhesion (e.g., immobilization of collagen, laminin and fibronectin onto the surface),[41] and different surface treatment methods to enhance the biocompatibility of, e.g., silicon.[43] Finally, it should be noted that it is important to establish a similar environment in the chip as in a standard cell incubator. In addition to temperature-control around 37 °C (discussed in Sect. II A), a 5% CO_2-level is appropriate for maintaining the correct pH level of the culture medium. Here, an open micro-device for acoustic manipulation of cells has the advantage of providing a simple method for temperature and CO_2 control directly at the liquid-gas interface.[17] In a closed system, CO_2 control can be implemented either by driving the system in perfusion mode or using a gas-permeable material such as PDMS. In a continuous-mode acoustophoretic microdevice, surface treatment and CO_2 control are of less importance since cells are only in the chip environment for times in the order of a few seconds. However, material choice and temperature stability are always important since they define the quality and stability of the acoustic resonance.

III Observed bioeffects on cells in ultrasonic standing wave manipulation devices

In an ultrasonic standing wave device, the bioeffects may be different from the effects of ultrasound in general. For example, cells in a water-based medium move by the acoustic radiation force[1] to the pressure nodes, while small (approx. a few μm in diameter or less) bubbles - if present or generated - typically move to the pressure antinodes at frequencies of a few MHz and at moderate amplitudes.[44] This means that potential cavitation

nuclei are physically separated from the cells in a standing wave. Furthermore, since cavitation threshold depends on the pressure amplitude, it is more likely that cavitation will occur in the pressure antinodes than in the pressure nodes. Thus, the radiation force in an ultrasonic standing wave actually provides a protective effect on cells. This implies that cells may be unaffected even if cavitation is present given that the field is of standing-wave type and that the size range of cavitation effects is less than the antinode-to-node distance $\lambda/4$ (approximately 0.4 mm at 1 MHz in water). Church commented on this protective effect on cells in standing-wave fields already in 1982 in a work on ultrasound-induced cell lysis.[45] He noticed that at moderate intensities (1 W cm^{-2}) and a frequency of 1 MHz, cell lysis was only efficient if the cell sample was rotated. Sample rotation led to a mixing of cells and bubbles that otherwise would have been separated into the node and antinodes, respectively, in the standing wave. However, it is well known that the motion of a bubble in a standing-wave field of a given frequency is dependent on the bubble size; bubbles smaller than a cut-off size (corresponding to the resonance frequency of the bubble) move to the pressure antinodes while bubbles larger than this cut-off size move to the pressure nodes.[46] For example, at 1 MHz, bubbles with diameter <7 μm move to the pressure antinodes while bubbles with diameter >7 μm move to the pressure node where the cells are trapped. Church predicted that the bubbles responsible for cavitation were those with sizes just below the resonance size, i.e., with diameter 4–7 μm at 1 MHz driving frequency. Even if larger bubbles may be present at the location of cells in the pressure nodes, they will most likely produce little or no damage to cells because (1) the pressure amplitude is very weak in the pressure node, and (2) the bubbles do not respond as strongly as they would if driven below resonance.[45] It should, however, be pointed out that bubble motion in a sound field is very complex. For example, at sufficiently high pressure amplitudes, active sub-resonant-size bubbles can behave like larger bubbles in a standing-wave field and accumulate in the pressure nodes, causing cell damage.[47,48,49]

A comparison of the impact on cellular viability between propagating fields and standing-wave fields was performed by Böhm *et al.*, who studied plant cells (*Petunia hybrida*) exposed to different energy densities, times and wave types of ultrasound.[50] The major finding from this study is seen in Fig. 4. For the stored energy density 8.5 J m^{-3}, and frequency around 2 MHz, practically no reduction in viability was observed for standing-wave exposure relative to the no-exposure control, while a dramatic reduction in viability was found during 20 min of propagating-wave exposure of the same magnitude. For standing-wave exposure, a reduction in viability was found for the stored energy densities 44 J m^{-3} and 70 J m^{-3} but still at a lower rate than for a propagating wave at 8.5 J m^{-3} stored energy density.[50] The authors concluded that the locations of cells in the pressure nodes of a standing-wave field correspond to positions of zero or low displacement gradient, where the latter is associated with mechanical stress. Thus, according to Böhm, for both displacement and pressure it is the field gradient and not magnitude that has a negative impact on the cells. Interestingly, Böhm also noted that cells in mitosis were more susceptible to mechanical stress and showed a lower viability than cells in other stages of the cell cycle.

Similar studies to Böhm's[50] were performed on yeast cells by Radel *et al.*[51,52] In agreement with Böhm's findings, Radel *et al.* noticed that cells agglomerated in the pressure nodal planes appeared to be less damaged by ultrasound than cells located elsewhere in a standing wave field or than cells located in a propagating wave field. However, although the cell membranes were intact and the cells were still viable, electron microscopy[51] and fluorescence microscopy[52] studies revealed morphological changes on intracellular structures when the yeast cells were exposed to <1 MPa and ~2 MHz standing-wave ultrasound. For example, the ultrasound seemed to disrupt the integrity of the vacuole membrane, but not the nucleus or plasma membranes. In agreement with Böhm's study, Radel *et al.* also noticed that the growth rate seemed to be hampered by ultrasound exposure, but only for cells that escaped from the pressure nodes. However, they suggested that this was due to intracellular damage of elements responsible for mitosis.[51] Furthermore, the ability to collect the yeast cells in the pressure nodal planes of the standing wave was dependent on the suspension properties: Yeast cells suspended in water was more strongly retained in the pressure nodes (and therefore less damaged) than yeast cells suspended in a water–ethanol mixture.[51] This result is of interest for systems using buffers that concentrates cells in the pressure anti-nodes; such systems may be less biocompatible than systems than concentrate cells in the pressure nodes.

A thorough study of the physical environment of neural-cell aggregates trapped by standing-wave ultrasound was performed by Bazou *et al.*[53] They concluded that in their device the cavitation threshold pressure amplitude was approx. 2 MPa, which is more than twice the pressure amplitude needed in most ultrasonic particle and cell manipulation devices. Furthermore, at 0.54 MPa pressure amplitude, an acoustic streaming velocity of 70 μm s^{-1} was measured, which corresponds to orders of magnitude lower level of hydrodynamic stress on cells compared to standard centrifugation at ~100–1000 *g* used routinely for cell culture preparation.

IV Methods for measuring the impact of ultrasound on cell viability

The most simple and straightforward method for quantifying the impact of ultrasound on cell viability in micro-scaled devices is to measure the integrity of the cell membrane by light microscopy. The thin cell membrane is one of the most fragile parts of the cell and also the boundary to the extracellular environment. Many of the physical mechanisms discussed in Sect II can rupture the cell membrane and it is therefore highly relevant to choose a membrane integrity-based method. The most commonly used dyes for viability studies in ultrasonic standing wave devices are trypan blue[54,55,56,57] and propidium iodide (PI).[58,59,60,61] Both these methods are based on dye exclusion, meaning that the dye is prevented
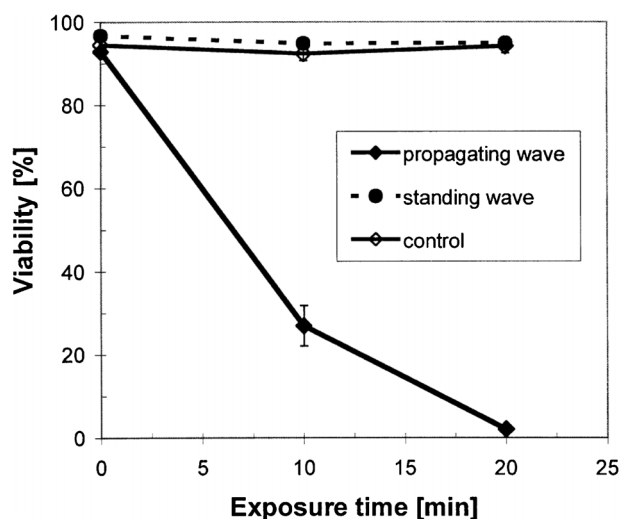

Fig. 4 Comparison of the cell viability of *Petunia hybrida* exposed to propagating-wave ultrasound and standing-wave ultrasound of equal stored energy densities (8.5 J m^{-3}, *n* = 2). The figure is reprinted from Böhm *et al.*[50] with permission from Elsevier.

from passing through the membranes of living cells. If the membrane is ruptured, the dye can traverse the plasma membrane and stain the cell. Trypan blue appears blue when illuminated with white light, while PI is a red-fluorescent dye used together with fluorescence microscopy settings. It should be noted that trypan blue has been reported to overestimate the viability, suggesting that fluorometric assays such as PI are more reliable.[62] An additional advantage with PI is that its fluorescence increases by a factor of ~ 30 when bound to nucleic acid, such as DNA in the nucleus. This means that there is practically no background fluorescence from PI outside the cells yielding a strong signal-to-noise ratio. On the other hand, PI is toxic for long incubation times. An alternative to the PI assay is the ethidium homodimer-1 (EthD-1) assay, which has been used for measuring the impact of ultrasonic standing waves on, for example, a liver cell line.[63] The opposite of the exclusion method is to use a dye that stains living but not dead cells, e.g. using the green-fluorescent (or orange-fluorescent) dye calcein AM.[17,42,58] Calcein AM (which initially is non-fluorescent), penetrates the membrane of living cells and the fluorescence is activated by an esterase-based enzymatic reaction present only in living cells. Thus, the green (or orange) fluorescence indicates two properties of a living cell: (1) That the cell has esterase activity and (2) that the esterase product (the fluorescent bi-product of calcein

AM) is retained within the cell, which means that the cell has an intact membrane. The latter is because the fluorescent form of calcein has much lower membrane permeability than the non-fluorescent form. When a cell dies, the fluorescence disappears primarily due to leakage of fluorescent calcein through the damaged membrane out from the cell. A similar method to the calcein AM assay is the acridine orange assay, which is based on a dye whose emission spectrum changes upon interaction with DNA and RNA in the cell. Evander et al. used this assay in a perfusion setting to monitor the viability of acoustically trapped neural stem cells in a microfluidic chip.[18] Recently, Augustsson et al. used the XTT assay to measure the mitochondrial dehydrogenase activity present in living cells from different prostate cancer cell lines with promising results.[64] A selection of different dyes that has been used for measuring viability of cells exposed to ultrasound is summarized in Table 1.

In fluorescence microscopy it is practical to use a combination of dyes, e.g. green-fluorescent calcein AM together with red-fluorescent PI. This way, all cells are clearly visible at all time points, either in green (live cells) or in red (dead cells), see Fig. 5. However, in this figure the red dye is not PI but far-red DDAO-SE. This is not a viability dye, but a cytoplasm dye which fluoresce independently on the viability state. During cell death the cells often go from green via

yellow (both colors visible) to red, which may reveal some information about the "death dynamics". It should be noted, however, that in viability assays based on PI or calcein AM, the definition of cell death is given by the assay principle. For example, in PI assays the definition of cell death is when PI binds to the nucleus, while in calcein AM assays the definition is either when the esterase-activated form of calcein leaks out through the damaged cell membrane, or (for already dead cells before the staining) that it has no esterase activity and therefore cannot produce the fluorescent form of calcein.

It is also possible to classify a cell as live or dead based on cell morphology. This can be seen in Fig. 5 where the "blebbing" of the cell membrane during programmed cell death, i.e. apoptosis, is shown. Here, blebbing means that the cell shape turns into a more irregular form with clear bulges or "blebs" in the membrane (see Fig. 5). These blebs, typical for early-stage apoptosis, can later detach from the cell, which finally breaks up into fragments (late-stage apoptosis), see Fig. 5. Apoptosis may be of interest in studies of delayed or long-term bioeffects of ultrasound on cells. For example, Bazou et al. studied the effect of early- and late-stage apoptosis of cells exposed to standing-wave ultrasound for up to 1 h.[58] For early-stage apoptosis, the fluorescence assay Annexin V-FITC was used, and for late-stage PI was used. The Annexin V assay is based on the translocation of the membrane

Table 1 Selected dyes used for measuring viability in ultrasonic cell manipulation devices

| Dye:	References:	Exclusion/inclusion method:	Indicator of:
Trypan blue	54,55,56,57	Stains dead cells	Damaged plasma membrane *Note: Not fluorescence-based*
Propidium iodide (PI)	58,59,60,61	Stains dead cells	Damaged plasma membrane *Note: Toxic for long incubation times*
Ethidium homodimer-1 (EthD-1)	63	Stains dead cells	Damaged plasma membrane *Note: Similar to PI*
Calcein AM	17,42,58	Stains living cells	Intact plasma membrane Esterase activity *Note: Compatible with long incubation times*
Acridine orange (AO)	18	Stains living cells (color-specific)	Cell cycle (emission spectrum depends on interaction with DNA and RNA)
XTT assay	64	Stains living cells	Mitochondrial dehydrogenase activity *Note: Colorimetric assay*
Annexin V-FITC	58	Stains apoptotic cells	Apoptosis (translocation of phosphatidylserine in the cell membrane)
Far-red DDAO-SE	72	Stains the cytoplasm (of both living and dead cells)	Must be used in combination with other dyes, e.g. calcein AM *Note: Compatible with very long incubation times*
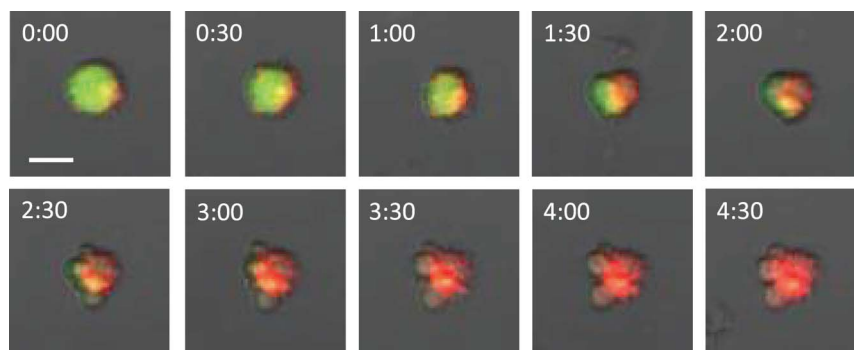
Fig. 5 A 4.5 h long time-lapse study of the dynamics of a human embryonic kidney cell (293T) undergoing apoptosis. The cell is labeled with calcein AM (green fluorescent) and far-red DDAO-SE (red-fluorescent). Both these dyes are compatible with long-term studies (approx. 12 h). The images show early (1:00–2:00 h) and late (2:30–4:30 h) apoptosis. The scale bar in the first image is 10 μm. The images are courtesy of Dr Bruno Vanherberghen.

phospholipid phosphatidylserine (PS) from the inner face of the plasma membrane to the cell surface, a process specific for early-stage apoptosis.[65] Morphology (blebbing) classification is a simple and straightforward alternative for measuring apoptosis, although it is more difficult to automate than fluorescence-based methods.

In addition to physical and visual attributes, such as membrane integrity and blebbing, viability can be measured indirectly by different means. In ultrasonic standing-wave devices, examples include measuring the release/leakage of naturally occurring intracellular components, such as potassium ions, haemoglobin and lactate dehydrogenase from erythrocytes.[66,67,68] Thus, if the membrane is damaged, the concentration of intracellular components outside the cells increases.[51] This method could be a better choice than using the different dyes discussed above since the dyes are not natural and may negatively affect the cells, particularly in long-term studies (>12 h). Another method was reported by Zhang et al., who measured protein expression and virus production in a baculovirus/insect cell expression system using an ultrasonic standing-wave cell retention device, compared to production levels without using ultrasound.[69] Similarly, in a standing-wave device of considerable power used for manipulation of a hybridoma culture, Chisti reported on a method where the rates of glucose uptake and antibody production were used as a viability measure.[70] Furthermore, the proliferation rate of different cell types exposed to standing-wave ultrasound has been used as a measure of delayed or long-term effects of ultrasonic exposure,

both in macro-[56,63,71] and micro-scale systems.[18,42,60] One interesting observation noticed by both Hultström[42] and Bazou[63] is the importance of cell–cell interaction for the maintenance of cell viability and growth rate. This seems to be important for adherent cells forming tissues such as kidney[42] and liver[63] cells. For example, the growth rate of ultrasonically aggregated kidney cells was higher than non-aggregated control cells in low-concentration samples, possibly due to the lack of cell–cell contact in the control sample not treated with ultrasound.[42]

The final work to be mentioned here is a recent paper by Dykes et al.[61] Instead of just measuring the direct viability, Dykes et al. also studied the functional impact of ultrasound on different blood cells after acoustophoretic separation in a microfluidic device. The functional tests included colony-forming ability of peripheral blood progenitor cells (PBPC) and activation levels of platelets. They concluded that the investigated cellular functions were preserved after the ultrasound exposure in their device.

V Conclusions

A general guideline when handling cells by ultrasound is to follow the same recommendation as James Bond's; a cell prefers to be shaken, not stirred. In a pressure node where cells are typically located in ultrasonic manipulation devices, the velocity of the fluid medium elements has a maximum while both the pressure and the pressure gradient have a minimum. Therefore, the cells are more shaken than squeezed, and most cavitation bubbles with the potential to cause shear stresses from fluid stirring or direct

damage to the cells are physically separated from the cells. Furthermore, any temperature increase from ultrasound can easily be limited and controlled. A viability-optimized ultrasonic manipulation device can manipulate cells for hours and days without any apparent negative impact on cellular state and growth.[17] However, few studies exist where cellular functions under the effect of long-term ultrasound exposure are investigated. One such example is a preliminary (several-hour exposure) study by Christakou et al., measuring the killing efficiency of natural killer cells aggregated with target cells using standing-wave ultrasound in a multi-well microplate.[72] In future it should be possible to use ultrasound either as a minimally influencing cell handling tool, or for triggering a cellular response, depending on the system design, operation and intended bio-application.

Acknowledgements

References

1 M. Settnes and H. Bruus, *Phys. Rev. E.*, 2012, **85**, 016327, 1–12.
2 W. L. Nyborg, *Ultrasound Med. Biol.*, 2000, **26**, 911–964.
3 M. C. Ziskin and D. B. Petitti, *Ultrasound Med. Biol.*, 1988, **14**, 91–96.
4 M. W. Miller, W. L. Nyborg, W. C. Dewey, M. J. Edwards, J. S. Abramowicz and A. A. Brayman, *Int. J. Hyperthermia*, 2002, **18**, 361–384.

5 S. B. Barnett, G. R. Ter Haar, M. C. Ziskin, W. T. Nyborg, K. Maeda and J. Bang, *Ultrasound Med. Biol.*, 1994, **20**, 205–218.

6 M. R. Bailey, V. A. Khokhlova, O. A. Sapozhnikov, S. G. Kargl and L. A. Crum, *Acoust. Phys.*, 2003, **49**, 437–464.

7 K. Richter, M. Haslbeck and J. Buchner, *Mol. Cell*, 2010, **40**, 253–266.

8 D. A. Walsh, N. W. Klein, L. E. Hightower and M. J. Edwards, *Teratology*, 1987, **36**, 181–191.

9 S. A. Sapareto and W. C. Dewey, *Int. J. Radiat. Oncol., Biol., Phys.*, 1984, **10**, 787–800.

10 D. M. Toivola, P. Strnad, A. Habtezion and M. B. Omary, *Trends Cell Biol.*, 2010, **20**, 79–91.

11 M. B. Al-Fageeh, R. J. Marchant, M. J. Carden and C. M. Smales, *Biotechnol. Bioeng.*, 2006, **93**, 829–835.

12 H. Kaufmann, X. Mazur, M. Fussenegger and J. E. Bailey, *Biotechnol. Bioeng.*, 1999, **63**, 573–582.

13 J. J. Hawkes and W. T. Coakley, *Enzyme Microb. Technol.*, 1996, **19**, 57–62.

14 K. A. J. Borthwick, W. T. Coakley, M. B. McDonnell, H. Nowotny, E. Benes and M. Gröschl, *J. Microbiol. Methods*, 2005, **60**, 207–216.

15 P. Augustsson, R. Barnkob, S. T. Wereley, H. Bruus and T. Laurell, *Lab Chip*, 2011, **11**, 4152–4164.

16 J. Svennebring, O. Manneberg and M. Wiklund, *J. Micromech. Microeng.*, 2007, **17**, 2469–2474.

17 B. Vanherberghen, O. Manneberg, A. Christakou, T. Frisk, M. Ohlin, H. M. Hertz, B. Önfelt and M. Wiklund, *Lab Chip*, 2010, **10**, 2727–2732.

18 M. Evander, L. Johansson, T. Lilliehorn, J. Piskur, M. Lindvall, S. Johansson, M. Almqvist, T. Laurell and J. Nilsson, *Anal. Chem.*, 2007, **79**, 2984–2991.

19 I. Z. Shirgaonkar, S. Lanthier and A. Kamen, *Biotechnol. Adv.*, 2004, **22**, 433–444.

20 R. E. Apfel, *J. Acoust. Soc. Am.*, 1997, **101**, 1227–1237.

21 M. Voltmer and A. Weber, *Z. Phys. Chem.*, 1926, **119**, 277–301.

22 R. E. Apfel and C. K. Holland, *Ultrasound Med. Biol.*, 1991, **17**, 179–185.

23 W. L. Nyborg, *Ultrasound Med. Biol.*, 2001, **3**, 301–333.

24 P. Marmottant and S. Hilgenfeldt, *Nature*, 2003, **423**, 153–156.

25 E. L. Carstensen, M.W. Miller and C. A. Linke, *J. Biol. Phys.*, 1974, **2**, 173–192.

26 D. L. Miller, R. M. Thomas and M. E. Frazier, *Ultrasound Med. Biol.*, 1991, **17**, 729–735.

27 K. S. Suslick, *Science*, 1990, **247**, 1439–1445.

28 J. R. Lindner, *Nat. Rev. Drug Discovery*, 2004, **3**, 527–532.

29 C. X. Deng, F. Sieling, H. Pan and J. Cui, *Ultrasound Med. Biol.*, 2004, **30**, 519–526.

30 C.-D. Ohl, M. Arora, R. Ikink, N. de Jong, M. Versluis, M. Delius and D. Lohse, *Biophys. J.*, 2006, **91**, 4285–4295.

31 S. Mitragotri, *Nat. Rev. Drug Discovery*, 2005, **4**, 255–260.

32 R. Karshafian, P. D. Bevan, R. Williams, S. Samac and P. N. Burns, *Ultrasound Med. Biol.*, 2009, **35**, 847–860.

33 W. Zhong, W. Hung Sit, J. M. F. Wan and A. C. H. Yu, *Ultrasound Med. Biol*, 2011, **37**, 2149–2159.

34 D. Carugo, D. N. Ankrett, P. Glynne-Jones, L. Capretto, R. J. Boltryk, P. A. Townsend, X. Zhang, M. Hill, *Proc. of μTAS* 2011, Seattle, USA, pp. 106–108.

35 M. Dyson, J. Pond and B. Woodward, *Nature*, 1971, **232**, 572–573.

36 M. Dyson, J. B. Pond, B. Woodward and J. Broadbent, *Ultrasound Med. Biol.*, 1974, **1**, 133–148.

37 E. S. B. C. Ang, V. Gluncic, A. Duque, M. E. Schafer and P. Rakic, *Proc. Natl. Acad. Sci. U. S. A.*, 2006, **103**, 12903–12910.

38 A. McQueen, E. Meilhoc and J. E. Bailey, *Biotechnol. Lett.*, 1987, **9**, 831–836.

39 D. E. Hughes and W. L. Nyborg, *Science*, 1962, **138**, 108–114.

40 S.-F. Chang, C. A. Chang, D.-Y. Lee, P.-L. Lee, Y.-M. Yeh, C.-R. Yeh, C.-K. Cheng, S. Chien and J.-J. Chiu, *Proc. Natl. Acad. Sci. U. S. A.*, 2008, **105**, 3927–3922.

41 L. Kim, Y.-C. Toh, J. Voldman and H. Yu, *Lab Chip*, 2007, **7**, 681–694.

42 J. Hultström, O. Manneberg, K. Dopf, H. M. Hertz, H. Brismar and M. Wiklund, *Ultrasound Med. Biol.*, 2007, **33**, 145–151.

43 T. W. Frisk, M. A. Khorshidi, K. Guldevall, B. Vanherberghen and B. Önfelt, *Biomed. Microdevices*, 2011, **4**, 683–693.

44 L. A. Crum and A. I. Eller, *J. Acoust. Soc. Am.*, 1970, **48**, 181–189.

45 C. C. Church, H. G. Flynn, M. W. Miller and P. G. Sacks, *Ultrasound Med. Biol.*, 1982, **8**, 299–309.

46 F. G. Blake, *J. Acoust. Soc. Am.*, 1949, **21**, 551.

47 T. Watanabe and Y. Kukita, *Phys. Fluids A*, 1993, **5**, 2682–2688.

48 A. A. Doinikov, *Phys. Fluids*, 2002, **14**, 1420–1425.

49 S. Khanna, N. N. Amso, S. J. Paynter and W. T. Coakley, *Ultrasound Med. Biol.*, 2003, **29**, 1463–1470.

50 H. Böhm, P. Anthony, M. R. Davey, L. G. Briarty, J. B. Power, K. C. Lowe, E. Benes and M. Gröschl, *Ultrasonics*, 2000, **38**, 629–632.

51 S. Radel, A. J. McLoughlin, L. Gherardini, O. Doblhoff-Dier and E. Benes, *Ultrasonics*, 2000, **38**, 633–637.

52 S. Radel, L. Gherardini, A. J. McLoughlin, O. Doblhoff-Dier and E. Benes, *Bioseparation*, 2001, **9**, 369–377.

53 D. Bazou, L. A. Kuznetsova and W. T. Coakley, *Ultrasound Med. Biol.*, 2005, **31**, 423–430.

54 D. G. Kilburn, D. J. Clarke, W. T. Coakley and D. W. Bardsley, *Biotechnol. Bioeng.*, 1989, **34**, 559–562.

55 O. Doblhoff-Dier, T. Gaida, H. Katinger, W. Burger, M. Gröschl and E. Benes, *Biotechnol. Prog.*, 1994, **10**, 428–432.

56 P. W. S. Pui, F. Trampler, S. A. Sonderhoff, M. Groeschl, D. G. Kilburn and J. M. Piret, *Biotechnol. Prog.*, 1995, **11**, 146–152.

57 Z. Wang, P. Grabenstetter, D. L. Feke and J. M. Belovich, *Biotechnol. Prog.*, 2004, **20**, 384–387.

58 D. Bazou, G. A. Foster, J. R. Ralphs and W. T. Coakley, *Mol. Membr. Biol.*, 2005, **22**, 229–240.

59 S. Khanna, B. Hudson, C. J. Pepper, N. N. Amso and W. T. Coakley, *Ultrasound Med. Biol.*, 2006, **32**, 289–295.

60 P. Thévoz, J. A. Adams, H. Shea, H. Bruus and T. Soh, *Anal. Chem.*, 2010, **82**, 3094–3098.

61 J. Dykes, A. Lenshof, I.-B. Åstrand-Grundström, T. Laurell and S. Scheding, *PLoS One*, 2011, **6**, e23074.

62 S. A. Altman, L. Randers and G. Rao, *Biotechnol. Prog.*, 1993, **9**, 671–674.

63 D. Bazou, W. T. Coakley, A. J. Hayes and S. K. Jackson, *Toxicol. in Vitro*, 2008, **22**, 1321–1331.

64 P. Augustsson, *On microchannel acousto-phoresis: Experimental considerations and life science applications*, Doctoral Thesis, Lund University, 2011.

65 S. J. Martin, C. P. M. Reutelingsperger, A. J. McGahon, J. A. Rader, R. C. A. A. van Schie, D. M. LaFace and D. R. Green, *J. Exp. Med.*, 1995, **182**, 1545–1556.

66 K. Yasuda, S. SW. Haupt and S. Umemura, *J. Acoust. Soc. Am.*, 1997, **102**, 642–645.

67 K. Yasuda, *Sens. Actuators, B*, 2000, **64**, 128–135.

68 C. M. Cousins, P. Holownia, J. J. Hawkes, M. S. Limaye, C. P. Price, P. J. Keay and W. T. Coakley, *Ultrasound Med. Biol.*, 2000, **26**, 881–888.

69 J. Zhang, A. Collins, M. Chen, I. Knyazev and R. Gentz, *Biotechnol. Bioeng.*, 1998, **59**, 351–359.

70 Y. Chisti, *Trends Biotechnol.*, 2003, **21**, 89–93.

71 L. Gherardini, C. M. Cousins, J. J. Hawkes, J. Spengler, S. Radel, H. Lawler, B. Devcic-Kuhar, M. Gröschl, W. T. Coakley and A. J. McLoughlin, *Ultrasound Med. Biol.*, 2005, **31**, 261–272.

72 A. E. Christakou, M. Ohlin, M. A. Khorshidi, B. Vanherberghen, B. Önfelt, M. Wiklund, *Proc. of μTAS* 2011, Seattle, USA.